0026-895X/10/7701-17–25$20.00
MOLECULAR PHARMACOLOGY
Vol. 77, No. 1
57877/3544981
Mol Pharmacol 77:17–25, 2010
Printed in U.S.A.

Epigallocatechin-3-gallate Inhibits Osteoclastogenesis by Down-Regulating c-Fos Expression and Suppressing the Nuclear Factor-κB Signal[S]

Jong-Ho Lee, Hexiu Jin, Hye-Eun Shim, Ha-Neui Kim, Hyunil Ha, and Zang Hee Lee

Department of Cell and Developmental Biology, Dental Research Institute, School of Dentistry, Seoul National University, Seoul, Republic of Korea

Received May 19, 2009; accepted October 14, 2009

ABSTRACT

Epigallocatechin-3-gallate (EGCG), the major anti-inflammatory compound in green tea, has been shown to suppress osteoclast differentiation. However, the precise molecular mechanisms underlying the inhibitory action of EGCG in osteoclastogenesis and the effect of EGCG on inflammation-mediated bone destruction remain unclear. In this study, we found that EGCG inhibited osteoclast formation induced by osteoclastogenic factors in bone marrow cell-osteoblast cocultures but did not affect the ratio of receptor activator of nuclear factor κB (NF-κB) ligand (RANKL) to osteoprotegerin induced by osteoclastogenic factors in osteoblasts. We also found that EGCG inhibited osteoclast formation from bone marrow macrophages (BMMs) induced by macrophage colony-stimulating factor plus RANKL in a dose-dependent manner without cytotoxicity. Pretreatment with EGCG significantly inhibited RANKL-induced the gene expression of c-Fos and nuclear factor of activated T-cells (NFATc1), essential transcription factors for osteoclast development. EGCG suppressed RANKL-induced activation of c-Jun N-terminal protein kinase (JNK) pathway, among the three well known mitogen-activated protein kinases and also inhibited RANKL-induced phosphorylation of the NF-κB p65 subunit at Ser276 and NF-κB transcriptional activity without affecting the degradation of IκBα and NF-κB DNA-binding in BMMs. The inhibitory effect of EGCG on osteoclast formation was somewhat reversed by retroviral c-Fos overexpression, suggesting that c-Fos is a downstream target for antiosteoclastogenic action of EGCG. In addition, EGCG treatment reduced interleukin-1-induced osteoclast formation and bone destruction in mouse calvarial bone in vivo. Taken together, our data suggest that EGCG has an antiosteoclastogenic effect by inhibiting RANKL-induced the activation of JNK/c-Jun and NF-κB pathways, thereby suppressing the gene expression of c-Fos and NFATc1 in osteoclast precursors.

Bone mass homeostasis is regulated by the coupled actions of bone-forming osteoblasts and bone-resorbing osteoclasts, a process termed remodeling. Many pathological and osteopenic diseases, including postmenopausal osteoporosis, lytic bone metastasis, rheumatoid arthritis, periodontitis, and Paget's disease, are characterized by progressive and excessive bone resorption by osteoclasts, which are multinucleated cells derived from the monocyte/macrophage linage precursors (Boyle et al., 2003). Macrophage colony-stimulating factor (M-CSF), which is produced by osteoblasts, plays an important role in proliferation and subsequent osteoclast differentiation in mouse bone marrow cultures (Biskobing et al., 1995). A tumor necrosis factor (TNF) family member, receptor activator of nuclear factor κB (NF-κB) ligand (RANKL), is

This work was supported by the Korea Health 21 Research and Development Project, Ministry of Health and Welfare, Republic of Korea [Grant A060480]; and the Science Research Center Grant to Bone Metabolism Research Center, Ministry of Education, Science and Technology [Grant 2009-0063264].

J.L. and H.J. contributed equally to this work.

Article, publication date, and citation information can be found at http://molpharm.aspetjournals.org.
doi:10.1124/mol.109.057877.

[S] The online version of this article (available at http://molpharm.aspetjournals.org) contains supplemental material.

ABBREVIATIONS: M-CSF, macrophage colony-stimulating factor; ALP, alkaline phosphatase; BMM, bone marrow macrophage; EGCG, epigallocatechin-3-gallate; EMSA, electrophoretic mobility shift assay; JNK, c-Jun N-terminal protein kinase; NFATc1, nuclear factor of activated T cells 1; NF-κB, nuclear factor κB; OC, osteoclast; OPG, osteoprotegerin; PBS, phosphate-buffered saline; PGE_2, prostaglandin E_2; RANKL, receptor activator of nuclear factor κB ligand; TNF, tumor necrosis factor; TRAP, tartrate-resistant acid phosphatase; $VitD_3$, 1,25-dihydroxyvitamin D_3; HEK, human embryonic kidney; ICAM, intercellular adhesion molecule; PCR, polymerase chain reaction; IL-1, interleukin 1; ERK, extracellular signal-regulated kinase; MEM, minimal essential medium; ICR, imprinting control region; HPRT, hypoxanthine-guanine phosphoribosyl transferase; ELISA, enzyme-linked immunosorbent assay; micro-CT, microcomputed tomography; SP600125, anthra[1,9-*c*,*d*]pyrazol-6(2*H*)-one; EGFP, enhanced green fluorescent protein.

expressed as a membrane-bound protein in osteoblasts and stromal cells or is released as a soluble factor by activated T-cells, which promotes osteoclast differentiation and activation (Takayanagi, 2007). Osteoblasts and stromal cells also produce a soluble decoy receptor for RANKL, osteoprotegerin (OPG), which inhibits osteoclast formation by interrupting the interaction between RANKL and RANK, resulting in an increase in bone density and bone volume (Simonet et al., 1997). Several osteoclastogenic factors, including 1,25-dihydroxyvitamin D_3 ($VitD_3$), parathyroid hormone, and proinflammatory cytokines, can stimulate osteoclast formation by up-regulating the ratio of RANKL to OPG in osteoblasts or stromal cells (Takayanagi, 2007). Thus, in many conditions, osteoclast formation is regulated directly or indirectly by environmental cells.

RANKL binding to RANK, a receptor of RANKL that is expressed in osteoclast precursors, mediates the biological effects of RANKL and leads to the recruitment of TNF receptor-associated factor 6, which results in the activation of downstream signaling pathways, including NF-κB, c-Jun N-terminal protein kinase (JNK), p38, ERK, and phosphatidylinositol 3-kinase/AKT (Darnay et al., 1998, 1999; Li et al., 2000; Lee et al., 2002). RANKL activation of JNK phosphorylates the transcription factor c-Jun (Kobayashi et al., 2001), which forms activator protein-1 complexes with c-Fos, an essential transcription factor for osteoclast formation (Grigoriadis et al., 1994). Genetic disruption experiments have revealed that mice lacking both of the p50 and p52 NF-κB subunits develop osteopetrosis caused by the arrested generation of osteoclasts (Franzoso et al., 1997; Iotsova et al., 1997). Thus, NF-κB genes play an indispensable role in regulating the differentiation and function of osteoclasts. It has been revealed that NF-κB functions upstream of c-Fos expression during RANKL-induced osteoclastogenesis. RANKL-induced c-Fos expression is abolished in NF-κB p50/p52 double-knockout osteoclast precursors, and RANKL can induce osteoclast formation from NF-κB p50/p52 double-knockout osteoclast precursors when c-Fos is overexpressed (Yamashita et al., 2007). Nuclear factor of activated T cells (NFATc1), which also plays an important role in osteoclastogenesis, is up-regulated by RANKL in osteoclast precursors through mechanisms that are dependent on NF-κB and c-Fos (Matsuo et al., 2004; Yamashita et al., 2007). Furthermore, overexpression of NFATc1 in osteoclast precursors causes proficient induction of osteoclast formation even without RANKL stimulation (Takayanagi et al., 2002). These discoveries imply that NFATc1 may be a master transcription factor for osteoclast differentiation.

Epigallocatechin-3-gallate (EGCG) is the major polyphenol in green tea. It has recently attracted interest for its emerging biological activities, such as antiarthritic, anti-inflammatory, and cancer chemoprevention effects, in a variety of experimental models (Ahmed et al., 2004, 2006; Doss et al., 2005). Furthermore, it has been reported that EGCG can induce the apoptotic cell death of osteoclasts (Nakagawa et al., 2002). Although EGCG has been shown to inhibit osteoclast formation (Yun et al., 2004), the precise molecular mechanisms of EGCG action remain unclear. In addition, whether EGCG has a therapeutic effect on pathological bone destruction has not been studied. In the present study, we investigated the effects of EGCG on osteoclast development and the molecular mechanisms for these effects in vitro and in vivo.

Materials and Methods

Reagents and Antibodies. Penicillin, streptomycin, α-MEM, and fetal bovine serum were purchased from Invitrogen (Carlsbad, CA). Recombinant soluble human M-CSF, human RANKL, mouse IL-1, and TNF-α were obtained from PeproTech (Rocky Hill, NJ). $VitD_3$, prostaglandin E_2 (PGE_2), and EGCG were purchased from Sigma-Aldrich (St. Louis, MO). SP600125 was from Calbiochem (La Jolla, CA). Specific antibodies for phospho-ERK1/2 (Thr202/Tyr204), ERK, phospho-JNK1/2 (Thr183/Tyr185), JNK, phospho-p38 (Thr180/Tyr182), p38, phospho-p65 (Ser536 and Ser276), p65, phospho-c-Jun (Ser73), c-Jun, phospho-AKT (Thr308 and Ser473), AKT, phospho-IκBα (Ser32), and IκBα were purchased from Cell Signaling Technology (Danvers, MA). Antibodies for c-Fos, NFATc1, and β-actin were purchased from Santa Cruz Biotechnology, Inc. (Santa Cruz, CA).

Preparation of Osteoclast Precursors. Mouse bone marrow cells were obtained from femurs and tibias of 5-week-old ICR mice and were incubated in α-MEM complete media containing 10% fetal bovine serum, 100 U/ml penicillin, and 100 μg/ml streptomycin on 10-cm culture dishes in the presence of M-CSF (10 ng/ml) overnight. Nonadherent bone marrow cells were transferred to 10-cm bacterial culture dishes and were cultured in the presence of M-CSF (30 ng/ml) for 3 days. Adherent cells were used as bone marrow macrophages (BMMs) as osteoclast precursors after nonadherent cells were washed out.

In Vitro Osteoclast Cultures. To generate osteoclasts, BMMs (4×10^4 cells/well) were cultured for 4 days with M-CSF (30 ng/ml) and RANKL (100 ng/ml) in 48-well (1 ml/well) tissue culture plates. To generate osteoclasts from the coculture of primary osteoblasts and bone marrow cells, primary osteoblasts from newborn ICR mouse calvariae were prepared as described previously (Ha et al., 2006). Bone marrow cells (3×10^5 cells/well) and primary osteoblasts (2.5×10^4 cells/well) were cocultured for 6 to 7 days in 1 ml of α-MEM complete medium in 48-well tissue culture plates. The complete medium was changed every third day. At the end of the culture period, the cells were fixed in 10% formalin for 10 min, permeabilized with 0.1% Triton X-100, and then stained for tartrate-resistant acid phosphatase (TRAP) by using the Leukocyte Acid Phosphatase Assay Kit (Sigma-Aldrich).

Cell Viability Assay. The XTT assay was performed to examine the effect of EGCG on the cytotoxicity of BMMs by using a Cell Proliferation Kit (Roche, Nutley, NJ) according to the manufacturer's instructions. BMMs (1×10^2 cells/well) were cultured with EGCG at various concentrations (1–50 μM) for 48 h in the presence of M-CSF (30 ng/ml) and RANKL (100 ng/ml) on 96-well plates (200 μl/well). Then, a medium containing 100 μl of XTT solution (XTT labeling reagent plus electron-coupling reagent) was added. After 6 h of incubation, the plate was read at 450 nm (650 nm reference) by using a 96-well plate recorder.

Western Blot Analysis. Cells were washed twice with ice-cold phosphate-buffered saline (PBS) and were lysed in lysis buffer containing 20 mM Tris-HCl, 150 mM NaCl, 1% Triton X-100, 0.2% deoxycholate, and protease and phosphatase inhibitors for 30 min on ice. Protein concentrations of cell lysates were determined by using the DC Protein Assay Kit (Bio-Rad Laboratories, Hercules, CA). An equal amount of proteins (30 μg/lane) was resolved by SDS-polyacrylamide gel electrophoresis and was then transferred to a polyvinylidene difluoride membrane (GE Healthcare, Chalfont St. Giles, Buckinghamshire, UK). The membrane was probed with the indicated primary antibody. Blots were finally developed by using horseradish peroxidase-conjugated secondary antibodies and were visualized by using enhanced chemiluminescence (enhanced chemiluminescence kit; GE Healthcare).

Nuclear Fraction and Electrophoretic Mobility-Shift Assay. Cells were washed twice with ice-cold PBS, lysed in buffer (50 mM Tris-HCl, pH 8.0, 2 mM EDTA, 0.5% Nonidet P-40, 20% glycerol, and 0.5 mM phenylmethylsulfonyl fluoride) for 5 min on ice, and were then microfuged at 1500*g* for 5 min. The pellet was lysed in buffer (20 mM HEPES, pH 7.6, 420 mM NaCl, 2 mM EDTA, 1% Triton X-100, 20% glycerol, 25 mM β-glycerophosphate, and 0.5 mM phenylmethylsulfonyl fluoride) for 30 min on ice and was then microfuged at 13,400*g* for 15 min. Supernatants were used as nuclear extracts. Electrophoretic mobility shift assay (EMSA) was performed as described previously (Lee et al., 2001). In brief, nuclear extracts (10 μg) were incubated with the reaction buffer [10 mM Tris-HCl, 50 mM KCl, 1 mM EDTA, 5% glycerol, 2 mM dithiothreitol, and 1 μg of poly(dI·dC)] containing approximately 20,000 cpm of ^{32}P-labeled NF-κB (5′-AGTTGAGGGGACTTTCCCAGGC-3′; Santa Cruz Biotechnology) binding site oligomer for 30 min at 20°C. The DNA-bound proteins were separated on 4%-polyacrylamide gels. The gels were dried and subjected to autoradiography.

Quantitative PCR Analysis. Total RNA was prepared by using an RNeasy Mini kit (QIAGEN, Valencia, CA) according to the manufacturer's instructions, and cDNA was synthesized from 2 μg of total RNA by use of reverse transcriptase (Superscript II Preamplification System; Invitrogen). Real-time PCR was performed on an ABI Prism 7500 sequence detection system with SYBR Green PCR Master Mix (Applied Biosystems, Warrington, Cheshire, UK) by following the manufacturer's protocols. The ABI 7500 sequence detector was programmed with the following PCR conditions: 40 cycles of 15 s of denaturation at 95°C, and 1 min of amplification at 60°C. All reactions were run in triplicate and were normalized to the housekeeping gene HPRT. Relative differences in PCR results were evaluated by using the comparative cycle threshold method. The following primer sets were used: mouse TNF-α: forward, 5′-GACGTGGAAGTGGCAGAAGAG-3′; reverse, 5′-TGCCACAAGCAGGAATGAGA-3′; mouse ICAM-1: forward, 5′-GCCTAAGGAAGACATGATA-3′; reverse, 5′-CAAGAAGAGTTGGGGACAAT-3′; mouse Nfkb2: forward, 5′-TACAAGCTGGCTGGTGGGGA-3′; reverse, 5′-GTCGCGGGTCTCAGGACCTT-3′; mouse c-Fos: forward, 5′-ACTTCTTGTTTCCGGC-3′; reverse, 5′-AGCTTCAGGGTAGGTG-3′; mouse NFATc1: forward, 5′-CCGTTGCTTCCAGAAAATAACA-3′; reverse, 5′-TGTGGGATGTGAACTCGGAA-3′; and mouse βHPRT: forward, 5′-CCTAAGATGAGCGCAAGTTGAA-3′; reverse, 5′-CCACAGGGACTAGAACACCTGCTA-3′.

RANKL and OPG Protein Expression Assays in Osteoblasts. Primary osteoblasts (4×10^5 cells/well) were pretreated with or without EGCG (20 μM) or vehicle (dimethyl sulfoxide) for 12 h and were then stimulated with IL-1 (10 ng/ml), TNF-α (20 ng/ml), and $VitD_3$ (10 nM) plus PGE_2 (100 nM) for 24 h. The amounts of RANKL proteins in cell lysate and OPG secretion in cell culture media were determined by using RANKL and OPG ELISA (R&D Systems, Minneapolis, MN) according to the manufacturer's instructions.

Retroviral Gene Transduction. The retroviral vectors pMX-IRES-EGFP and pMX-c-Fos-IRES-EGFP were kindly provided by Dr. Nacksung Kim (University of Chonnam, Gwangju, Korea). Retrovirus packaging was performed by transient transfection of these pMX vectors into Plat-E retroviral packaging cells (Cell Biolabs, San Diego, CA). After incubation in fresh medium for 2 days, culture supernatants of the retrovirus-producing cells were collected. For retroviral infection, nonadherent bone marrow cells were cultured in M-CSF (30 ng/ml) for 48 h. Media were removed and replaced with culture supernatants of pMX-IRES-EGFP and pMX-c-Fos-IRES-EGFP virus-producing Plat-E cells together with hexadimethrine bromide (Polybrene; 6 μg/ml) and M-CSF (30 ng/ml) for 12 h. Infected cells were then cultured in the presence of M-CSF for 1 day and then further cultured with or without EGCG (20 μM) in the presence of M-CSF (30 ng/ml) and RANKL (100 ng/ml) for 4 days.

Luciferase Reporter Assays. HEK293T cells were plated at a density of 5×10^4 cells/well in 24-well plates. The next day, cells were transfected with 0.8 μg of RANK and NF-κB luciferase reporter vector by using 2 μl of Lipofectamine 2000 (Invitrogen) for 6 h in Dulbecco's modified Eagle's medium, and then the medium was replaced by Dulbecco's modified Eagle's complete medium. After incubation for 12 h at 37°C in 5% CO_2, the cells were pretreated with EGCG (20 μM) or vehicle (dimethyl sulfoxide) for 12 h and were then stimulated with RANKL (100 ng/ml) for the indicated times. The cells were lysed in Reporter Lysis Buffer (Promega, Madison, WI), and luciferase activity was measured by using a luminometer (EG&G Berthold, Bad Wildbad, Germany).

In Vivo Experiments. An IL-1-induced mouse calvarial bone loss model was used as described previously (Ha et al., 2006). In brief, a collagen sponge treated with vehicle (PBS) or IL-1 (2 μg) was implanted over calvarial bone in groups of 10 mice (6-week-old male ICR mice). Mice were intraperitoneally administered EGCG (15 μg/g of body weight) or vehicle (dimethyl sulfoxide) daily beginning on day 0. The mice were sacrificed 7 days after the implantation, and whole calvariae were fixed in 4% paraformaldehyde and stained for TRAP. Three-dimensional images of calvarial bone were obtained by microcomputed tomography (micro-CT) scanning (SMX-90CT; Shimadzu Corporation, Kyoto, Japan). Bone mineral content was determined by using TRI 3D-BON (RACTOC System Engineering Co., Tokyo, Japan) program. For histological analysis, calvarial tissues were fixed in 4% paraformaldehyde, decalcified in 12% EDTA, and then embedded in paraffin. After that, histological sections (5 μm) were prepared, stained for TRAP, and counterstained by using hematoxylin. Image analysis (Image J, National Institutes of Health; http://rsbweb.nih.gov/ij/) was further used to quantify the osteoclasts number and the percentage of osteoclast surface. All animal experiments were reviewed and approved by the Seoul National University School of Dentistry Animal Care Committee (Seoul, Korea).

Statistical Analysis. Values are presented as the mean ± S.D. values from three or more experiments. Data were analyzed with the Student's *t* test for comparisons between two mean values. A value of $P < 0.05$ was considered significant.

Results

EGCG Suppresses Osteoclast Formation in Bone Marrow Cell-Osteoblast Cocultures and Primary BMMs. We first examined the effect of EGCG on osteoclast formation induced by osteoclastogenic factors in cocultures of bone marrow cells and primary osteoblasts in vitro. Stimulation of IL-1 (10 ng/ml), TNF-α (20 ng/ml), and $VitD_3$ (10 nM), plus PGE_2 (100 nM) for 6 days formed TRAP-positive multinucleated osteoclasts in the cocultures and, under these conditions, treatment with EGCG (at 20 μM) significantly inhibited osteoclast formation (Fig. 1A). In these culture systems, osteoblasts support osteoclastogenesis from osteoclast precursors by regulating the expression of RANKL and OPG (Takayanagi, 2007). We thus evaluated by ELISA whether EGCG affects the expression of RANKL and OPG in osteoblasts. The addition of osteoclastogenic factors, including IL-1, TNF-α, and $VitD_3$ plus PGE_2, increased RANKL expression and decreased OPG expression at 24 h in osteoblasts. Pretreatment with EGCG did not alter the expression of RANKL or OPG (Fig. 1B). We next examined the effects of EGCG on RANKL-induced osteoclast formation from osteoclast precursor BMMs. RANKL (100 ng/ml) generated numerous TRAP-positive multinucleated osteoclasts in the presence

of M-CSF (30 ng/ml) for 4 days. Treatment of the same cultures with EGCG suppressed osteoclast formation in a dose-dependent manner (Fig. 1C). Complete inhibition of osteoclast formation was achieved with 20 μM EGCG, and this concentration was subsequently used unless otherwise noted. The antiosteoclastogenic effect of EGCG was not mediated through cellular toxicity or cell proliferation, even at high doses (50 μM) (Fig. 1D).

EGCG Down-Regulates c-Fos and NFATc1 Expression Induced by RANKL. To determine the molecular mechanisms of the action of EGCG in osteoclastogenesis, we first examined the effect of EGCG on the expression of the key transcription factors, c-Fos and NFATc1. As reported previously, the expression of c-Fos and NFATc1 was up-regulated in BMMs by RANKL stimulation. Pretreatment with EGCG for 12 h strongly inhibited the RANKL-induced mRNA expression of c-Fos and NFATc1 (Fig. 2A) and also suppressed RANKL-induced the two protein expression in a dose-dependent manner (Fig. 2, B and C). To investigate whether c-Fos is a downstream target for the antiosteoclastogenic action of EGCG, we ectopically expressed the c-Fos gene in BMMs by use of a retroviral system. By forced expression of c-Fos (Fig. 2D), the inhibitory effect of EGCG on RANKL-induced osteoclast formation was somewhat reversed (Fig. 2E).

EGCG Inhibits the RANKL-Induced Phosphorylation of JNK and c-Jun in BMMs. To further investigate the molecular mechanisms underlying the inhibitory effects of EGCG on RANKL-induced c-Fos expression and osteoclast formation, we examined the effects of EGCG on RANKL-induced early signaling pathways including ERK, JNK, p38, and AKT. Phosphorylation of these signaling molecules was observed at 5 min after RANKL treatment in BMMs. Among these pathways, phosphorylation of JNK and its downstream target c-Jun was only suppressed by pretreatment with EGCG (Fig. 3A). Thus, we examined whether JNK/c-Jun activation is required for RANKL-induced c-Fos induction in BMMs. Pretreatment of BMMs with SP600125, a specific JNK inhibitor, at 5 μM suppressed RANKL-induced JNK phosphorylation and subsequent c-Jun phosphorylation (Fig. 3B) without changing in RANKL-induced p-ERK, p-p38, p-Akt, and p-IκBα levels (data not shown). Moreover, the RANKL-induced expression of the key transcription factors c-Fos and NFATc1 was inhibited by SP600125 (Fig. 3C). Consistent with these effects, osteoclast formation was strongly suppressed (Fig. 3D).

EGCG Inhibits RANKL-Induced NF-κB Transcriptional Activity without Affecting Its DNA Binding Activity. RANKL stimulation leads to the activation of NF-κB, mitogen-activated protein kinases, and AKT (Darnay et al.,

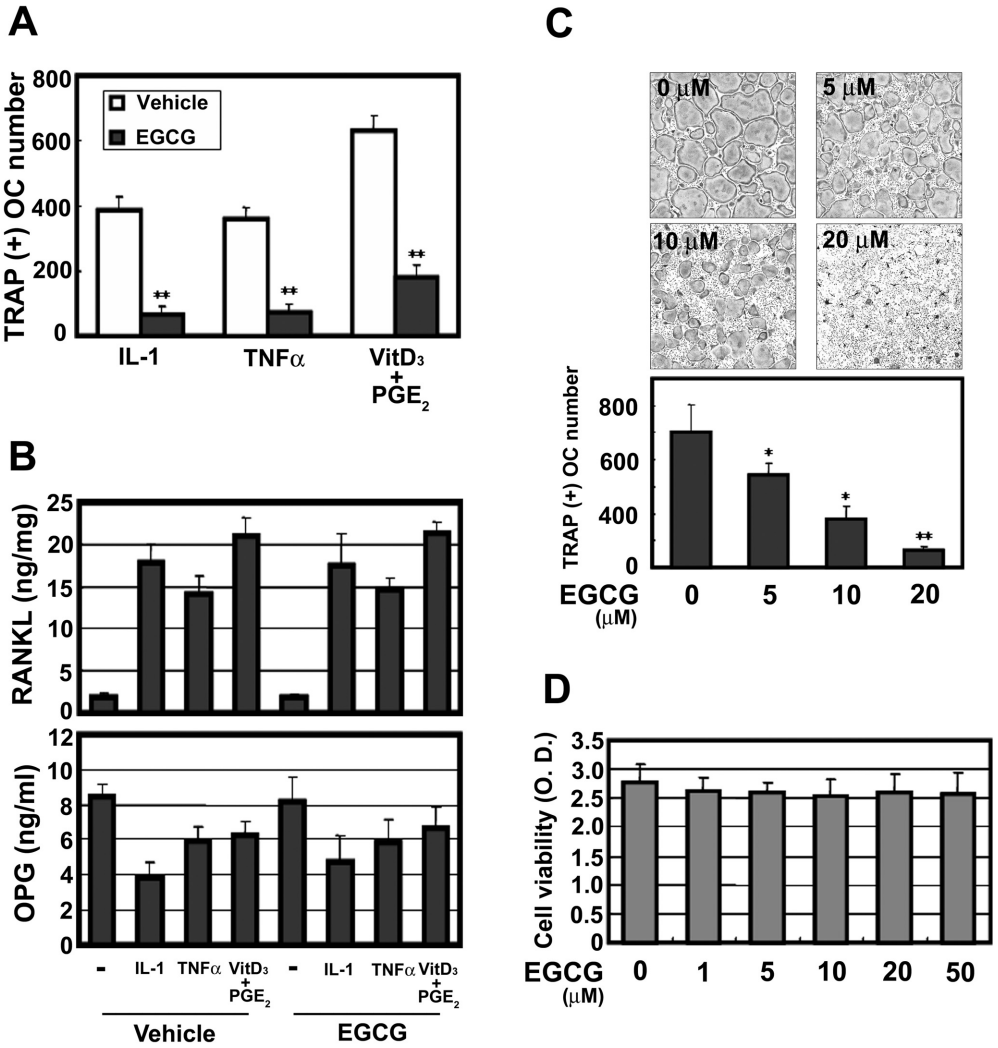

Fig. 1. EGCG inhibits osteoclast formation from cocultures and BMMs. A, mouse bone marrow cells and primary osteoblasts were cocultured with IL-1 (10 ng/ml), TNF-α (20 ng/ml), or $VitD_3$ (10 nM) plus PGE_2 (100 nM) in the presence of EGCG (20 μM) or vehicle (dimethyl sulfoxide) for 6 days. After culturing, the generated osteoclasts were detected by TRAP staining, and TRAP-positive multinucleated cells containing three or more nuclei were counted as osteoclasts (OCs) (**, $P < 0.01$). B, mouse primary osteoblasts were pretreated with EGCG (20 μM) or vehicle (dimethylsulfoxide) for 12 h and then were stimulated with IL-1 (10 ng/ml), TNF-α (20 ng/ml), or $VitD_3$ (10 nM) plus PGE_2 (100 nM) for 24 h. The amounts of RANKL and OPG were determined by using ELISA kits in cell lysates and in cell culture media, respectively. C, BMMs were cultured with M-CSF (30 ng/ml) and RANKL (100 ng/ml) at the indicated doses of EGCG for 4 days. After culturing, cells were fixed, and TRAP staining was performed (top). The number of TRAP-positive multinucleated OCs was counted (bottom) (*, $P < 0.05$; **, $P < 0.01$ versus untreated control). D, BMMs were cultured for 48 h with M-CSF (30 ng/ml) and RANKL (100 ng/ml) at the indicated doses of EGCG. Then, cell viability was determined by XTT assay as described under *Materials and Methods*.

1998, 1999; Li et al., 2000; Lee et al., 2002). Thus, we next assessed the effect of EGCG on RANKL-induced NF-κB activation. In HEK293T cells cotransfected with RANK and an NF-κB reporter gene, simulation of RANKL augmented NF-κB transcriptional activation, which was significantly inhibited by EGCG treatment (Fig. 4A). To examine whether EGCG inhibits RANKL-induced NF-κB-dependent transcription in BMMs, we evaluated mRNA levels of several NF-κB-regulated genes by using real-time quantitative PCR. There was an increase in ICAM-1, Nfkb2, and TNF-α mRNA expression after RANKL stimulation. Consistent with the results of NF-κB reporter assay, pretreatment with EGCG lessened RANKL-induced up-regulation of these genes (Fig. 4B). The primary regulatory point of NF-κB activity is at the level of IκB protein degradation. RANKL stimulation led to the phosphorylation and almost complete degradation of IκBα within 15 min, as assessed by Western blotting and pretreatment with EGCG did not alter either phosphorylation or degradation of IκBα (Fig. 4C). Furthermore, EGCG did not impair the RANKL-stimulated DNA-binding activity of NF-κB in the EMSA assay (Fig. 4D). It is noteworthy that we found that EGCG inhibits RANKL-stimulated phosphorylation of the NF-κB p65 subunit at Ser276 but not Ser536 (Fig. 4C), which has been shown to be involved in NF-κB transcriptional activity (Vermeulen et al., 2003; Dong et al., 2008).

EGCG Prevents IL-1-Induced Osteoclast Formation and Bone Destruction In Vivo. Finally, having established that EGCG inhibits osteoclastogenesis in vitro, we addressed whether the same effect could be observed in vivo. TRAP staining of whole calvariae and histological sections showed that IL-1 dramatically increased osteoclast number and surface (Fig. 5, A, D, and E). In parallel with the effects in vitro, EGCG notably reduced IL-1-induced osteoclast formation when administered systemically. Furthermore, the results of the bone histomorphometric analysis after micro-CT also showed that IL-1-induced bone destruction was notably prevented by EGCG treatment (Fig. 5, B and C).

Discussion

Excessive RANKL signaling causes enhanced osteoclast formation and bone resorption. As such, the down-regulation of RANKL expression or its downstream signals may be a valuable approach to the treatment of pathological bone loss. In the present study, we found that EGCG prevents osteoclast differentiation from bone marrow cells and primary osteoblast cocultures induced by IL-1, TNF-α, and $VitD_3$ plus PGE_2 without affecting the expression of RANKL and OPG. We next investigated whether EGCG inhibits RANKL-induced osteoclast formation from its precursors in the absence of osteoblasts or stromal cells. As reported previously (Yun et al., 2004), TRAP-positive multinuclear cells from this culture were decreased in a dose-dependent manner after treatment with EGCG, which was similar to the observations in cocultures. These results clearly suggest that EGCG suppresses osteoclast formation by directly acting on osteoclast precursors.

Several transcription factors, including PU.1, microphthalmia-associated transcription factor, NF-κB, c-Fos, and NFATc1 have been shown to play a role in osteoclast development from its precursors. PU.1 and microphthalmia-associated transcription factor mediate the early nonspecific differentiation along the osteoclast pathway (Teitelbaum and Ross, 2003), whereas NF-κB, c-Fos, and NFATc1 function downstream of RANKL signaling for osteoclast differentia-

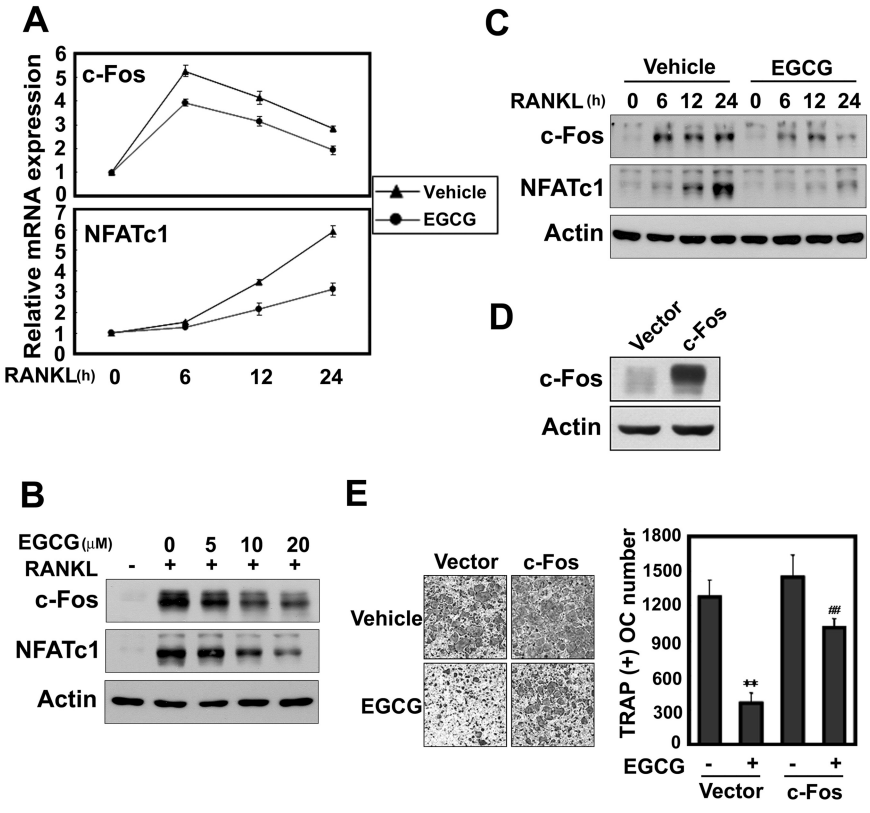

Fig. 2. EGCG suppresses RANKL-induced expression of c-Fos and NFATc1 in BMMs. A and C, BMMs were pretreated with EGCG (20 μM) or vehicle (dimethyl sulfoxide) in the presence of M-CSF for 12 h and then were stimulated with RANKL (100 ng/ml) for the indicated times. B, BMMs were pretreated with EGCG (5–20 μM) or vehicle (dimethyl sulfoxide) in the presence of M-CSF for 12 h and then were stimulated with RANKL for 24 h. The expression of mRNA for c-Fos and NFATc1 was analyzed by real-time PCR with HPRT mRNA as an endogenous control (A). Western blotting was performed with the indicated antibodies (B and C). Actin served as an internal control. D and E, BMMs were infected with retroviruses expressing pMX-IRES-EGFP (Vector) or pMX-c-Fos-EGFP (c-Fos). Infected BMMs were cultured for 24 h, and Western blotting was performed for c-Fos expression levels (D). Infected BMMs were cultured with or without EGCG (20 μM) in the presence of M-CSF (30 ng/ml) and RANKL (100 ng/ml) for 4 days. After culturing, the cells were fixed, and the cells were stained for TRAP (E, left). TRAP-positive multinucleated OCs were counted (E, right; **, $P < 0.01$, versus untreated control; ##, $P < 0.01$, versus Vector group treated with EGCG).

tion. The c-Fos/c-Jun/NFATc1 pathway plays a critical and essential role in osteoclast development, and the lack of any of these three components arrests osteoclastogenesis (Teitelbaum, 2004). In this study, RANKL-induced expression of c-Fos and NFATc1 was dramatically down-regulated with EGCG pretreatment. Furthermore, the forced expression of c-Fos somewhat reversed the EGCG inhibition of osteoclastogenesis, suggesting that c-Fos is a target of the EGCG inhibitory effect on osteoclast development.

Stimulation of RANKL has been reported to activate three well known mitogen-activated protein kinases: ERK, JNK, and p38. Furthermore, each specific inhibitor of mitogen-activated protein kinase kinase and p38 or dominant-negative JNK prevented RANKL-induced osteoclastogenesis, which suggest that these signaling pathways also have a role in osteoclast formation (Kobayashi et al., 2001; Lee et al., 2002; Ikeda et al., 2004). We found that pretreatment with EGCG specifically down-regulates the JNK activation without affecting the activation of ERK and p38. In JNK pathway, MKK7, one of the major JNK upstream kinases, is involved in osteoclastogenesis (Yamamoto et al., 2002; Ikeda et al., 2004), and c-Jun, the best-characterized substrates of JNK, is also required for maximum induction of NFATc1 and osteoclastogenesis in response to RANKL (Ikeda et al., 2004). In our experiments, EGCG inhibited RANKL-induced c-Jun phosphorylation (Fig. 3A) but not MKK7 phosphorylation (data not shown). We also found that blockade of the JNK/c-Jun pathway by the JNK inhibitor SP600125 not only impaired RANKL-induced osteoclast formation but also inhibited RANKL-induced c-Fos and NFATc1 expression. Taken together, these results strongly suggest that EGCG suppresses RANKL-induced osteoclast differentiation and the induction of c-Fos and NFATc1 at least in part by inhibiting JNK/c-Jun pathway in BMMs.

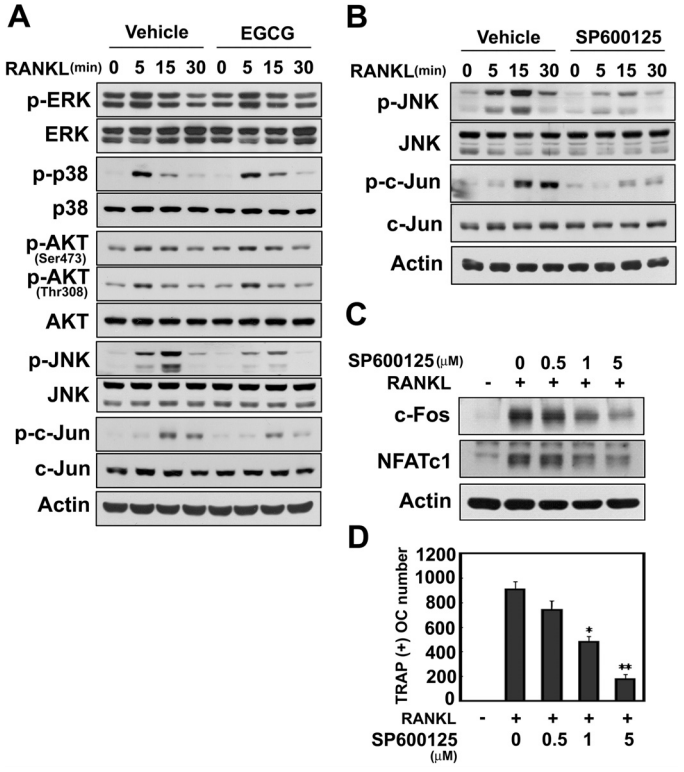

Fig. 3. EGCG down-regulates the JNK/c-Jun pathway in BMMs. A, BMMs were pretreated with EGCG (20 μM) or vehicle (dimethyl sulfoxide) for 12 h in the presence of M-CSF (30 ng/ml) and were then stimulated with RANKL (100 ng/ml) for the indicated times. Whole-cell lysates were subjected to Western blotting with the indicated antibodies. Actin served as an internal control. B, BMMs were pretreated with SP600125 (5 μM) or vehicle (dimethyl sulfoxide) for 3 h in the presence of M-CSF (30 ng/ml) and were then stimulated with RANKL (100 ng/ml) for the indicated times. Whole-cell lysates were subjected to Western blotting with the indicated antibodies. Actin served as an internal control. C, BMMs were pretreated with SP600125 (0.5–5 μM) or vehicle (dimethyl sulfoxide) for 3 h and were then stimulated with RANKL for 24 h. Western blotting was performed with the indicated antibodies. Actin served as an internal control. D, BMMs were cultured with M-CSF (30 ng/ml) and RANKL (100 ng/ml) at the indicated doses of SP600125 for 4 days. After culturing, cells were fixed, and TRAP staining was performed. The number of TRAP-positive multinucleated OCs was counted (*, $P < 0.05$; **, $P < 0.01$ versus untreated control).

The crucial role of NF-κB signaling in osteoclast development has been demonstrated by genetic experiments, including p50/p52 NF-κB double-knockout mice that displayed severe osteopetrosis (Franzoso et al., 1997; Iotsova et al., 1997) and inhibitory κB kinase β knockout mice that exhibited failed osteoclastogenesis (Ruocco et al., 2005). It has been suggested that NF-κB functions upstream of c-Fos expression during RANKL-induced osteoclastogenesis (Yamashita et al., 2007). Similar to the JNK/c-Jun pathway, NF-κB also seems to be involved in RANKL-induced NFATc1 induction and c-Fos induction. Takatsuna et al. (2005) showed that an NF-κB inhibitor suppresses RANKL-stimulated induction of NFATc1. In addition, NF-κB cooperates with NFATc2 to activate the initial induction of NFATc1, followed by an autoamplification of NFATc1 (Asagiri et al., 2005). In this study, EGCG inhibited RANKL-induced NF-κB transcriptional activation, suggesting that the down-regulation of NF-κB-dependent transcription might be involved in the inhibitory effect of EGCG on RANKL induction of c-Fos and NFATc1 during osteoclastogenesis.

NF-κB proteins can be post-translationally modified, including acetylation (Chen et al., 2001), *S*-nitrosylation (Marshall et al., 2004), and phosphorylation (Zhong et al., 1998; Vermeulen et al., 2002, 2003), which can affect NF-κB activity. It has been shown that phosphorylation of the NF-κB p65 subunit at Ser276 plays a critical role for TNF-induced transactivation of p65 and acts as a switch regulating the association with either cAMP response element-binding protein-binding protein/p300 or histone deacetylase (Zhong et al., 1998, 2002; Vermeulen et al., 2003). Dong et al. (2008) showed that cells from a knock-in mouse containing the nonphosphorylatable p65 S276A variant display a significant reduction of some but not all NF-κB-responsive gene expression without affecting DNA binding activity, and that unphosphorylated nuclear NF-κB can affect the expression of genes not normally regulated by NF-κB through epigenetic mechanisms. In this study, RANKL stimulated both phosphorylation of the p65 subunit at Ser276 and Ser536. It is interesting that EGCG specifically inhibited RANKL-induced phosphorylation of the p65 subunit at Ser276 but not at Ser536. Thus, these results may imply that RANKL-induced phosphorylation of the p65 subunit at Ser276 plays a role in the osteoclastic gene induction by NF-κB transcription-dependent and/or -independent mechanisms. However, further studies are required to clarify this possibility.

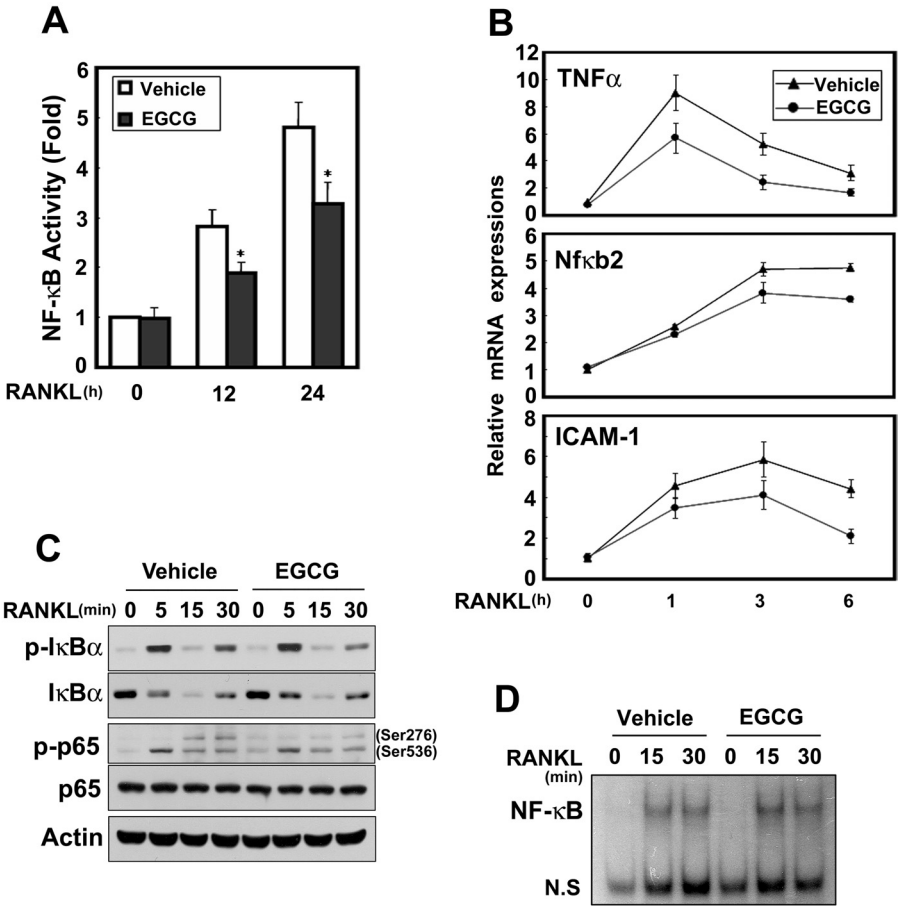

Fig. 4. EGCG impairs RANKL-induced transcriptional activity of NF-κB in BMMs. A, HEK293T cells were cotransfected with RANK and NF-κB-luciferase plasmid. At 12 h after transfection, the cells were pretreated with EGCG (20 μM) or vehicle (dimethyl sulfoxide) for 12 h and were then stimulated with RANKL (100 ng/ml) for the indicated times. Cells were lysed, and the luciferase activity was determined by using a luciferase reporter assay system (*, $P < 0.05$ versus untreated control). B, BMMs were pretreated with EGCG (20 μM) or vehicle (dimethyl sulfoxide) in the presence of M-CSF for 12 h and then stimulated with RANKL (100 ng/ml) for the indicated times. Expression of mRNA for TNF-α, Nfkb2, and ICAM-1 was analyzed by real-time PCR using HPRT mRNA as an endogenous control. C, BMMs were pretreated with EGCG (20 μM) or vehicle (dimethyl sulfoxide) for 12 h in the presence of M-CSF (30 ng/ml) and then stimulated with RANKL (100 ng/ml) for the indicated time points. The phosphorylation of IκBα and p65 (Ser276 and Ser536) were detected with specific antibodies. D, BMMs were pretreated EGCG (20 μM) or vehicle (dimethyl sulfoxide) for 12 h in the presence of M-CSF (30 ng/ml) and then stimulated with RANKL (100 ng/ml) for 15 or 30 min. Cells were harvested, and nuclear extracts were prepared. DNA binding activity of NF-κB was assessed by EMSA. N.S., nonspecific band.

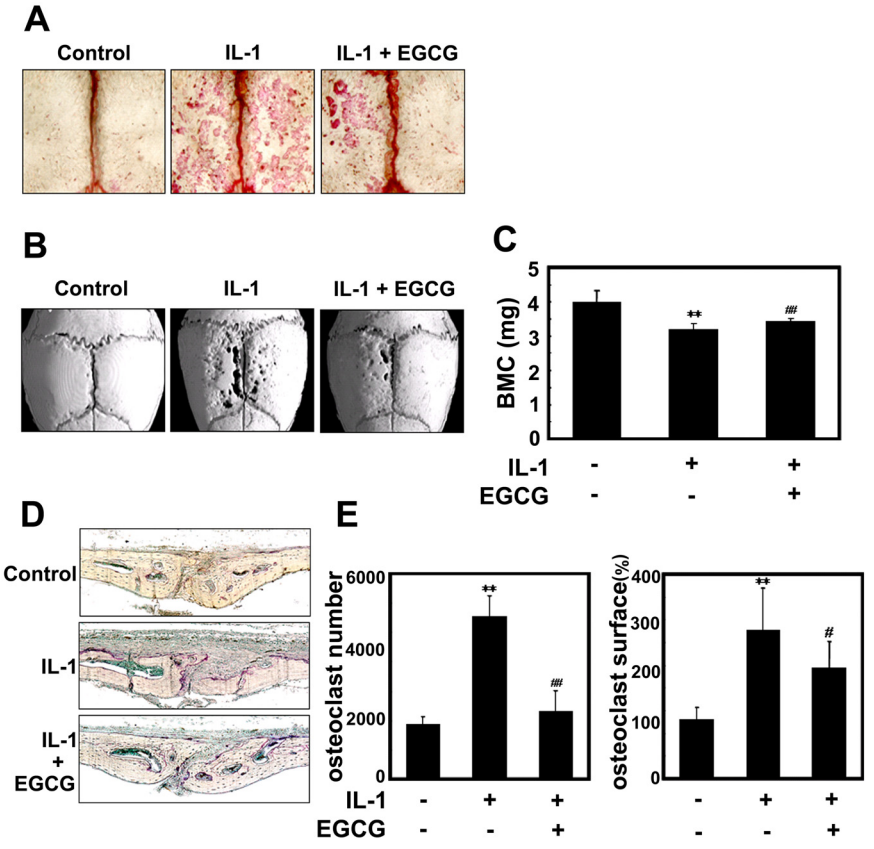

Fig. 5. Therapeutic value of EGCG on IL-1-induced bone destruction in vivo. A collagen sponge treated with vehicle (PBS) or IL-1 (2 μg) was implanted over 6-week-old mouse calvaria. EGCG (15 μg/g body weight) or vehicle (dimethyl sulfoxide) was administered intraperitoneally daily. The mice were sacrificed 7 days after implantation. A, TRAP staining of whole calvaria. Three-dimensional images of calvarial bone by micro-CT analysis were presented (B), and bone mineral content was measured (C; **, $P < 0.01$ versus untreated control; ##, $P < 0.01$ versus group treated with IL-1 only). Histological sections of calvarial bone were TRAP-stained with hematoxylin counterstaining (D), and osteoclast number (left)/surface (right) was analyzed (E; left, **, $P < 0.01$ versus untreated control; ##, $P < 0.01$ versus group treated with IL-1 only; right, **, $P < 0.01$ versus untreated control; #, $P < 0.05$ versus group treated with IL-1 only).

IL-1 is a proinflammatory cytokine that is believed to be a potent stimulator of the pathological bone destruction induced by both estrogen deficiency and inflammation. Mice lacking the type I IL-1 receptor are resistant to bone destruction after ovariectomy (Lorenzo et al., 1998). Blocking IL-1 signaling can also reduce bone loss and cartilage degradation in animal models of rheumatoid arthritis (Abramson and Amin, 2002). In our experiments, EGCG noticeably suppressed IL-1-induced calvarial bone destruction and osteoclast formation in vivo. The in vivo effects are most likely the result of the suppression of RANKL induction of c-Fos and NFATc1 in osteoclast precursors.

Bone homeostasis depends on maintaining a delicate balance between bone resorption by osteoclasts and bone formation by osteoblasts (Boyle et al., 2003). Thus, we next examined the effects of EGCG on bone formation by primary mouse calvarial osteoblasts. Osteogenic media containing ascorbic acid, β-glycerophosphate, and BMP2 substantially promoted alkaline phosphatase (ALP) activity (Supplemental Fig. S1A) and bone nodule formation as shown by alizarin red-S (Supplemental Fig. S1B). Treatment of osteoblasts with EGCG up to 20 μM did not affect ALP activity, while showing a marginal effect on bone nodule formation at 20 μM (Supplemental Fig. S1, A and B). Consistent with ALP activity, the mRNA levels of osteoblast marker genes Runx2, ALP, and Osteocalcin (Owen et al., 1990; Ducy et al., 1997; Murshed et al., 2005) were not affected by EGCG treatment (Supplemental Fig. S1C).

In summary, our findings clearly show that EGCG has an antiosteoclastogenic potential by reducing RANKL induction of c-Fos and NFATc1 in osteoclast precursors. The inhibitory action of EGCG on RANKL-induced activation of NF-κB and JNK/c-Jun pathways is most likely involved in this antiosteoclastogenic effect. EGCG also prevented IL-1-induced osteoclastic bone destruction in vivo. Thus, our findings strongly suggest that EGCG deserves new evaluation as a potential treatment option in various bone diseases associated with excessive osteoclast formation and bone destruction.

References

Abramson SB and Amin A (2002) Blocking the effects of IL-1 in rheumatoid arthritis protects bone and cartilage. *Rheumatology (Oxford)* **41:**972–980.

Ahmed S, Pakozdi A, and Koch AE (2006) Regulation of interleukin-1beta-induced chemokine production and matrix metalloproteinase 2 activation by epigallocatechin-3-gallate in rheumatoid arthritis synovial fibroblasts. *Arthritis Rheum* **54:** 2393–2401.

Ahmed S, Wang N, Lalonde M, Goldberg VM, and Haqqi TM (2004) Green tea polyphenol epigallocatechin-3-gallate (EGCG) differentially inhibits interleukin-1β-induced expression of matrix metalloproteinase-1 and -13 in human chondrocytes. *J Pharmacol Exp Ther* **308:**767–773.

Asagiri M, Sato K, Usami T, Ochi S, Nishina H, Yoshida H, Morita I, Wagner EF, Mak TW, Serfling E, et al. (2005) Autoamplification of NFATc1 expression determines its essential role in bone homeostasis. *J Exp Med* **202:**1261–1269.

Biskobing DM, Fan X, and Rubin J (1995) Characterization of MCSF-induced proliferation and subsequent osteoclast formation in murine marrow culture. *J Bone Miner Res* **10:**1025–1032.

Boyle WJ, Simonet WS, and Lacey DL (2003) Osteoclast differentiation and activation. *Nature* **423:**337–342.

Chen Lf, Fischle W, Verdin E, and Greene WC (2001) Duration of nuclear NF-kappaB action regulated by reversible acetylation. *Science* **293:**1653–1657.

Darnay BG, Haridas V, Ni J, Moore PA, and Aggarwal BB (1998) Characterization of the intracellular domain of receptor activator of NF-κB (RANK). Interaction with tumor necrosis factor receptor-associated factors and activation of NF-κB and c-Jun N-terminal kinase. *J Biol Chem* **273:**20551–20555.

Darnay BG, Ni J, Moore PA, and Aggarwal BB (1999) Activation of NF-κB by RANK requires tumor necrosis factor receptor-associated factor (TRAF) 6 and NF-κB-inducing kinase. Identification of a novel TRAF6 interaction motif. *J Biol Chem* **274:**7724–7731.

Dong J, Jimi E, Zhong H, Hayden MS, and Ghosh S (2008) Repression of gene expression by unphosphorylated NF-kappaB p65 through epigenetic mechanisms. *Genes Dev* **22:**1159–1173.

Doss MX, Potta SP, Hescheler J, and Sachinidis A (2005) Trapping of growth factors by catechins: a possible therapeutical target for prevention of proliferative diseases. *J Nutr Biochem* **16:**259–266.

Ducy P, Zhang R, Geoffroy V, Ridall AL, and Karsenty G (1997) Osf2/Cbfa1: a transcriptional activator of osteoblast differentiation. *Cell* **89:**747–754.

Franzoso G, Carlson L, Xing L, Poljak L, Shores EW, Brown KD, Leonardi A, Tran T, Boyce BF, and Siebenlist U (1997) Requirement for NF-kappaB in osteoclast and B-cell development. *Genes Dev* **11:**3482–3496.

Grigoriadis AE, Wang ZQ, Cecchini MG, Hofstetter W, Felix R, Fleisch HA, and Wagner EF (1994) c-Fos: a key regulator of osteoclast-macrophage lineage determination and bone remodeling. *Science* **266:**443–448.

Ha H, Lee JH, Kim HN, Kim HM, Kwak HB, Lee S, Kim HH, and Lee ZH (2006) alpha-Lipoic acid inhibits inflammatory bone resorption by suppressing prostaglandin E2 synthesis. *J Immunol* **176:**111–117.

Ikeda F, Nishimura R, Matsubara T, Tanaka S, Inoue J, Reddy SV, Hata K, Yamashita K, Hiraga T, Watanabe T, et al. (2004) Critical roles of c-Jun signaling in regulation of NFAT family and RANKL-regulated osteoclast differentiation. *J Clin Invest* **114:**475–484.

Iotsova V, Caamaño J, Loy J, Yang Y, Lewin A, and Bravo R (1997) Osteopetrosis in mice lacking NF-kappaB1 and NF-kappaB2. *Nat Med* **3:**1285–1289.

Kobayashi N, Kadono Y, Naito A, Matsumoto K, Yamamoto T, Tanaka S, and Inoue J (2001) Segregation of TRAF6-mediated signaling pathways clarifies its role in osteoclastogenesis. *EMBO J* **20:**1271–1280.

Lee SE, Chung WJ, Kwak HB, Chung CH, Kwack KB, Lee ZH, and Kim HH (2001) Tumor necrosis factor-alpha supports the survival of osteoclasts through the activation of Akt and ERK. *J Biol Chem* **276:**49343–49349.

Lee SE, Woo KM, Kim SY, Kim HM, Kwack K, Lee ZH, and Kim HH (2002) The phosphatidylinositol 3-kinase, p38, and extracellular signal-regulated kinase pathways are involved in osteoclast differentiation. *Bone* **30:**71–77.

Li J, Sarosi I, Yan XQ, Morony S, Capparelli C, Tan HL, McCabe S, Elliott R, Scully S, Van G, et al. (2000) RANK is the intrinsic hematopoietic cell surface receptor that controls osteoclastogenesis and regulation of bone mass and calcium metabolism. *Proc Natl Acad Sci U S A* **97:**1566–1571.

Lorenzo JA, Naprta A, Rao Y, Alander C, Glaccum M, Widmer M, Gronowicz G, Kalinowski J, and Pilbeam CC (1998) Mice lacking the type I interleukin-1 receptor do not lose bone mass after ovariectomy. *Endocrinology* **139:**3022–3025.

Marshall HE, Hess DT, and Stamler JS (2004) S-nitrosylation: physiological regulation of NF-κB. *Proc Natl Acad Sci U S A* **101:**8841–8842.

Matsuo K, Galson DL, Zhao C, Peng L, Laplace C, Wang KZ, Bachler MA, Amano H, Aburatani H, Ishikawa H, et al. (2004) Nuclear factor of activated T-cells (NFAT) rescues osteoclastogenesis in precursors lacking c-Fos. *J Biol Chem* **279:**26475–26480.

Murshed M, Harmey D, Millán JL, McKee MD, and Karsenty G (2005) Unique coexpression in osteoblasts of broadly expressed genes accounts for the spatial restriction of ECM mineralization to bone. *Genes Dev* **19:**1093–1104.

Nakagawa H, Wachi M, Woo JT, Kato M, Kasai S, Takahashi F, Lee IS, and Nagai K (2002) Fenton reaction is primarily involved in a mechanism of (−)-epigallocatechin-3-gallate to induce osteoclastic cell death. *Biochem Biophys Res Commun* **292:**94–101.

Owen TA, Aronow M, Shalhoub V, Barone LM, Wilming L, Tassinari MS, Kennedy MB, Pockwinse S, Lian JB, and Stein GS (1990) Progressive development of the rat osteoblast phenotype in vitro: reciprocal relationships in expression of genes associated with osteoblast proliferation and differentiation during formation of the bone extracellular matrix. *J Cell Physiol* **143:**420–430.

Ruocco MG, Maeda S, Park JM, Lawrence T, Hsu LC, Cao Y, Schett G, Wagner EF, and Karin M (2005) I{kappa}B kinase (IKK){beta}, but not IKK{alpha}, is a critical mediator of osteoclast survival and is required for inflammation-induced bone loss. *J Exp Med* **201:**1677–1687.

Simonet WS, Lacey DL, Dunstan CR, Kelley M, Chang MS, Lüthy R, Nguyen HQ, Wooden S, Bennett L, Boone T, et al. (1997) Osteoprotegerin: a novel secreted protein involved in the regulation of bone density. *Cell* **89:**309–319.

Takatsuna H, Asagiri M, Kubota T, Oka K, Osada T, Sugiyama C, Saito H, Aoki K, Ohya K, Takayanagi H, et al. (2005) Inhibition of RANKL-induced osteoclastogenesis by (−)-DHMEQ, a novel NF-kappaB inhibitor, through downregulation of NFATc1. *J Bone Miner Res* **20:**653–662.

Takayanagi H (2007) Osteoimmunology: shared mechanisms and crosstalk between the immune and bone systems. *Nat Rev Immunol* **7:**292–304.

Takayanagi H, Kim S, Koga T, Nishina H, Isshiki M, Yoshida H, Saiura A, Isobe M, Yokochi T, Inoue J, et al. (2002) Induction and activation of the transcription factor NFATc1 (NFAT2) integrate RANKL signaling in terminal differentiation of osteoclasts. *Dev Cell* **3:**889–901.

Teitelbaum SL (2004) RANKing c-Jun in osteoclast development. *J Clin Invest* **114:**463–465.

Teitelbaum SL and Ross FP (2003) Genetic regulation of osteoclast development and function. *Nat Rev Genet* **4:**638–649.

Vermeulen L, De Wilde G, Notebaert S, Vanden Berghe W, and Haegeman G (2002) Regulation of the transcriptional activity of the nuclear factor-kappaB p65 subunit. *Biochem Pharmacol* **64:**963–970.

Vermeulen L, De Wilde G, Van Damme P, Vanden Berghe W, and Haegeman G (2003) Transcriptional activation of the NF-kappaB p65 subunit by mitogen- and stress-activated protein kinase-1 (MSK1). *EMBO J* **22:**1313–1324.

Yamamoto A, Miyazaki T, Kadono Y, Takayanagi H, Miura T, Nishina H, Katada T, Wakabayashi K, Oda H, Nakamura K, et al. (2002) Possible involvement of IkappaB kinase 2 and MKK7 in osteoclastogenesis induced by receptor activator of nuclear factor kappaB ligand. *J Bone Miner Res* **17:**612–621.

Yamashita T, Yao Z, Li F, Zhang Q, Badell IR, Schwarz EM, Takeshita S, Wagner EF, Noda M, Matsuo K, et al. (2007) NF-κB p50 and p52 regulate receptor activator of NF-κB ligand (RANKL) and tumor necrosis factor-induced osteoclast precursor differentiation by activating c-Fos and NFATc1. *J Biol Chem* **282:** 18245–18253.

Yun JH, Pang EK, Kim CS, Yoo YJ, Cho KS, Chai JK, Kim CK, and Choi SH (2004) Inhibitory effects of green tea polyphenol (−)-epigallocatechin gallate on the expression of matrix metalloproteinase-9 and on the formation of osteoclasts. *J Periodontal Res* **39:**300–307.

Zhong H, May MJ, Jimi E, and Ghosh S (2002) The phosphorylation status of nuclear NF-kappa B determines its association with CBP/p300 or HDAC-1. *Mol Cell* **9:**625–636.

Zhong H, Voll RE, and Ghosh S (1998) Phosphorylation of NF-kappa B p65 by PKA stimulates transcriptional activity by promoting a novel bivalent interaction with the coactivator CBP/p300. *Mol Cell* **1:**661–671.

Address correspondence to: Dr. Zang Hee Lee, Department of Cell and Developmental Biology, School of Dentistry, Seoul National University, 28 Yeongon-Dong, Jongro-Gu, Seoul 110-749, Republic of Korea. E-mail: zang1959@snu.ac.kr